

# Baryon Stopping and Charged Particle Distributions in Central Pb+Pb Collisions at 158 GeV per Nucleon

H. Appelshäuser<sup>7,#</sup>, J. Bächler<sup>5</sup>, S.J. Bailey<sup>16</sup>, L.S. Barnby<sup>3</sup>, J. Bartke<sup>6</sup>, R.A. Barton<sup>3</sup>, H. Białkowska<sup>14</sup>, A. Billmeier<sup>10</sup>, C.O. Blyth<sup>3</sup>, R. Bock<sup>7</sup>, B. Boimska<sup>14</sup>, C. Bormann<sup>10</sup>, F.P. Brady<sup>8</sup>, R. Brockmann<sup>7,†</sup>, R. Brun<sup>5</sup>, P. Bunčić<sup>5,10</sup>, H.L. Caines<sup>3</sup>, D. Cebra<sup>8</sup>, G.E. Cooper<sup>2</sup>, J.G. Cramer<sup>16</sup>, P. Csato<sup>4</sup>, J. Dunn<sup>8</sup>, V. Eckardt<sup>13</sup>, F. Eckhardt<sup>12</sup>, M.I. Ferguson<sup>5</sup>, H.G. Fischer<sup>5</sup>, D. Flierl<sup>10</sup>, Z. Fodor<sup>4</sup>, P. Foka<sup>10</sup>, P. Freund<sup>13</sup>, V. Friese<sup>12</sup>, M. Fuchs<sup>10</sup>, F. Gabler<sup>10</sup>, J. Gal<sup>4</sup>, R. Ganz<sup>13</sup>, M. Gaździcki<sup>10</sup>, W. Geist<sup>13</sup>, E. Gładysz<sup>6</sup>, J. Grebieszko<sup>15</sup>, J. Günther<sup>10</sup>, J.W. Harris<sup>17</sup>, S. Hegyi<sup>4</sup>, T. Henkel<sup>12</sup>, L.A. Hill<sup>3</sup>, I. Huang<sup>2,8</sup>, H. Hümmeler<sup>10,+</sup>, G. Igo<sup>11</sup>, D. Irmscher<sup>2,7</sup>, P. Jacobs<sup>2</sup>, P.G. Jones<sup>3</sup>, K. Kadija<sup>18,13</sup>, V.I. Kolesnikov<sup>9</sup>, M. Kowalski<sup>6</sup>, B. Lasiuk<sup>11,17</sup>, P. Lévai<sup>4</sup>, A.I. Malakhov<sup>9</sup>, S. Margetis<sup>2,8</sup>, C. Markert<sup>7</sup>, G.L. Melkumov<sup>9</sup>, A. Mock<sup>13</sup>, J. Molnár<sup>4</sup>, J.M. Nelson<sup>3</sup>, M. Oldenburg<sup>10</sup>, G. Odyniec<sup>2</sup>, G. Palla<sup>4</sup>, A.D. Panagiotou<sup>1</sup>, A. Petridis<sup>1</sup>, A. Piper<sup>12</sup>, R.J. Porter<sup>2</sup>, A.M. Poskanzer<sup>2</sup>, S. Poziońska<sup>10</sup>, D.J. Prindle<sup>16</sup>, F. Pühlhofer<sup>12</sup>, J.G. Reid<sup>16</sup>, R. Renfordt<sup>10</sup>, W. Retyk<sup>15</sup>, H.G. Ritter<sup>2</sup>, D. Röhrich<sup>10</sup>, C. Roland<sup>7</sup>, G. Roland<sup>10</sup>, H. Rudolph<sup>2,10</sup>, A. Rybicki<sup>6</sup>, A. Sandoval<sup>7</sup>, H. Sann<sup>7</sup>, A.Yu. Semenov<sup>9</sup>, E. Schäfer<sup>13</sup>, D. Schmiscke<sup>10</sup>, N. Schmitz<sup>13</sup>, S. Schönfelder<sup>13</sup>, P. Seyboth<sup>13</sup>, F. Sikler<sup>4</sup>, E. Skrzypczak<sup>15</sup>, G.T.A. Squier<sup>3</sup>, R. Stock<sup>10</sup>, H. Ströbele<sup>10</sup>, I. Szentpetery<sup>4</sup>, J. Sziklai<sup>4</sup>, M. Toy<sup>2,11</sup>, T.A. Trainor<sup>16</sup>, S. Trentalange<sup>11</sup>, T. Ullrich<sup>17</sup>, M. Vassiliou<sup>1</sup>, G. Vesztegombi<sup>4</sup>, D. Vranic<sup>5,18</sup>, F. Wang<sup>2</sup>, D.D. Weerasundara<sup>16</sup>, S. Wenig<sup>5</sup>, C. Whitten<sup>11</sup>, T. Wienold<sup>2,#</sup>, L. Wood<sup>8</sup>, N. Xu<sup>2</sup>, T.A. Yates<sup>3</sup>, J. Zimanyi<sup>4</sup>, X.-Z. Zhu<sup>16</sup>, R. Zybert<sup>3</sup>  
(NA49 Collaboration)

<sup>1</sup>Department of Physics, University of Athens, Athens, Greece

<sup>2</sup>Lawrence Berkeley National Laboratory, University of California, Berkeley, USA

<sup>3</sup>Birmingham University, Birmingham, England

<sup>4</sup>KFKI Research Institute for Particle and Nuclear Physics, Budapest, Hungary

<sup>5</sup>CERN, Geneva, Switzerland

<sup>6</sup>Institute of Nuclear Physics, Cracow, Poland

<sup>7</sup>Gesellschaft für Schwerionenforschung (GSI), Darmstadt, Germany

<sup>8</sup>University of California at Davis, Davis, USA

<sup>9</sup>Joint Institute for Nuclear Research, Dubna, Russia

<sup>10</sup>Fachbereich Physik der Universität, Frankfurt, Germany

<sup>11</sup>University of California at Los Angeles, Los Angeles, USA

<sup>12</sup>Fachbereich Physik der Universität, Marburg, Germany

<sup>13</sup>Max-Planck-Institut für Physik, Munich, Germany

<sup>14</sup>Institute for Nuclear Studies, Warsaw, Poland

<sup>15</sup>Institute for Experimental Physics, University of Warsaw, Warsaw, Poland

<sup>16</sup>Nuclear Physics Laboratory, University of Washington, Seattle, WA, USA

<sup>17</sup>Yale University, New Haven, CT, USA

<sup>18</sup>Rudjer Boskovic Institute, Zagreb, Croatia

(October 4, 2018)

Net proton and negative hadron spectra for central Pb+Pb collisions at 158 GeV per nucleon at the CERN SPS were measured and compared to spectra from lighter systems. Net baryon distributions were derived from those of net protons. Stopping and mean transverse momentum  $\langle p_T \rangle$  of net baryons increase with system size. The rapidity density of negative hadrons scales with the number of participant nucleons for nuclear collisions, whereas their  $\langle p_T \rangle$  is independent of system size. The  $\langle p_T \rangle$  systematics are consistent with larger transverse flow velocity at midrapidity for Pb+Pb compared to S+S central collisions.

PACS numbers: 25.75-q, 25.75.Dw

Lattice QCD predicts that strongly interacting matter at an energy density greater than 1-2 GeV/fm<sup>3</sup> attains a deconfined, chirally restored state known as the quark-

gluon plasma (for an overview, see [1]). This state of matter existed in the early universe, and it may influence the dynamics of rotating neutron stars [2]. The collision of nuclei at ultrarelativistic energies offers the possibility in the laboratory of creating strongly interacting matter at sufficiently high energy density to form a quark gluon plasma [3]. Hadronic spectra from these reactions reflect the dynamics of the hot and dense zone formed in the collision. The baryon density, established early in the reaction, is an important factor governing the evolution of the system [4]. Comparison of model predictions with experimental rapidity and transverse momentum distributions and correlation functions constrains the possible dynamical scenarios of the reaction [5], such as those for longitudinal and transverse flow [6]. In addition, the mechanism by which the incoming nucleons lose momentum during the collision (baryon stopping [7]) is an important theoretical problem [8–10], and the measurement of baryon

stopping in heavy ion collisions provides essential data on this question.

In this paper, we present measurements by the NA49 collaboration of rapidity and transverse momentum distributions of participating baryons and negative hadrons over a large fraction of phase space for central Pb+Pb collisions at 158 GeV per nucleon ( $\sqrt{s_{NN}} = 17.2$  GeV). Hadronic spectra from S+S collisions at 200 GeV per nucleon [11–13] and N+N (nucleon-nucleon) collisions at 200 and 400 GeV [14,15] serve as important references, helping to identify effects that depart from those expected from the linear superposition of many N+N collisions.

The NA49 apparatus is described in [16]. A beam of  $^{208}\text{Pb}$  ions at 158 GeV per nucleon ( $y_{lab} = 5.8$ ) from the CERN SPS struck a 224 mg/cm<sup>2</sup> thick natural Pb target. The 5% most central collisions were selected by measurement of the forward-going energy in the phase space occupied by the projectile spectator nucleons. The reaction products passed through a dipole magnetic field, and tracks from charged particles used for this analysis were measured in two large Main Time Projection Chambers (MTPCs) placed downstream of the magnets on either side of the beam axis. Over 1000 tracks were measured in each event. Identification of protons utilized the specific ionization ( $\langle dE/dx \rangle$ ) of the gas of the MTPC [17]. A relative  $\langle dE/dx \rangle$  resolution of 6% was achieved.

The evolution of the incoming baryons (baryon stopping) was studied through measurement of the difference of the proton and antiproton distributions (net protons, denoted  $p-\bar{p}$ ) to eliminate the effect of baryon-antibaryon pair production. Meson production was studied through the yield of negative hadrons ( $h^-$ ), comprising primarily  $\pi^-$ , with an admixture of  $K^-$  and  $\bar{p}$ .  $5 \times 10^4$  central events were used for the  $p-\bar{p}$  analysis and  $7 \times 10^3$  central events were used for the  $h^-$  analysis.

The net proton yield was determined by a novel technique [18] in which the distribution of  $\langle dE/dx \rangle$  from negatively charged particles was subtracted from that of positively charged particles in narrow bins in  $(y, p_T)$ , and two Gaussian functions (net protons and pions) were fitted to the resulting extrema in each difference distribution. A correction to the net proton yield for the difference between  $K^+$  and  $K^-$  yields, based upon preliminary NA49 data [19], was 15% at  $y_{cm} < 0$  and was negligible for  $y_{cm} > 1$ . The negative hadron yield was determined from the yield of all tracks from negatively charged particles excluding electrons, identified via  $\langle dE/dx \rangle$ .

Corrections for detector acceptance and track reconstruction efficiency were calculated by embedding and reconstructing simulated tracks in real events [18]. The tracking efficiency was greater than 95% over most of the acceptance, falling below 80% in regions of high track density and near the edges of the acceptance. Yield as a function of rapidity was determined only for bins having full  $p_T$  coverage, except for the two lowest bins for  $h^-$ , where extrapolation was based upon the adjacent bin having full coverage. Instrumental background due

to secondary interactions with detector material was estimated, using a GEANT-based Monte Carlo simulation and the VENUS event generator [10], to be 5% of the total measured yield. Excluding the decay corrections discussed below, the systematic errors of all rapidity distributions were less than 10%.

The measured yields contain contributions from the products of weak decays that were incorrectly reconstructed as primary vertex tracks. This background correction to the  $h^-$  yield, primarily due to the decay of  $K_S^0$ , was estimated using preliminary NA49 data [19] to be 15% at midrapidity, decreasing strongly at higher rapidity. The background correction to the  $p-\bar{p}$  yield is due to the decays of  $\Lambda$  and  $\bar{\Lambda}$  (including  $\Sigma^0$  and feeddown from weak decays),  $\Sigma^+$ , and  $\bar{\Sigma}^+$ . To investigate the dependence of this correction on the phase space distribution of the decaying particles, three different rapidity distributions for  $\Lambda-\bar{\Lambda}$  were used, based upon (I) predictions of the RQMD model [9] and (II) the VENUS model [10], and (III) a preliminary NA49 measurement [19]. In each case the  $\Sigma^+ - \bar{\Sigma}^+$  yield was assumed to be 30% of the  $\Lambda - \bar{\Lambda}$  yield and to have the same rapidity distribution. For consistency with the charged kaon distribution used in the correction for proton identification and to conserve total strangeness, the hyperon yields in I and II were scaled by the ratio of total charged kaon yields in the data and the model. In III, the  $\Lambda + \Sigma^0$  rapidity distribution was scaled such that the ratio of  $\Lambda + \Sigma^0$  to charged kaon total yield agreed with that from both models.

Fig. 1, upper panel, shows the event normalized net proton yield as a function of rapidity for central Pb+Pb collisions incorporating  $\Lambda-\bar{\Lambda}$  corrections I, II and III (data points and errors shown only for I), and the corresponding  $\Lambda-\bar{\Lambda}$  rapidity distributions. Also shown is the proton rapidity distribution for p+p collisions at 400 GeV [15], which is qualitatively different. The comparison highlights the importance of multiple collisions to baryon stopping in nuclear collisions.

To determine the net baryon ( $B-\bar{B}$ ) rapidity distribution, the contribution of the remaining net baryons, in addition to  $p-\bar{p}$  and  $\Lambda-\bar{\Lambda}$ , must be included. Model calculations [9,10] indicate that the rapidity distribution of net neutrons follows that of net protons over most of phase space, with a 7% larger yield. The contribution to  $B-\bar{B}$  from charged hyperons was accounted for by assuming a common rapidity distribution for all net hyperons and scaling the  $\Lambda-\bar{\Lambda}$  distribution by an empirical factor 1.6 derived from hadronic reactions [20]. The net baryon yield  $B-\bar{B}$  was then calculated as

$$B-\bar{B} = (2.07 \pm 0.05) \cdot (p-\bar{p}) + (1.6 \pm 0.1) \cdot (\Lambda-\bar{\Lambda}). \quad (1)$$

Fig. 1, lower panel, shows the  $B-\bar{B}$  rapidity distribution for Pb+Pb. The data points and errors are for  $\Lambda-\bar{\Lambda}$  distribution I. The variation in  $B-\bar{B}$  due to the use of different  $\Lambda-\bar{\Lambda}$  distributions is smaller than that due to other sources of systematic error. Also shown in Fig. 1, lower panel, is the  $B-\bar{B}$  rapidity distribution for the 3%

most central S+S collisions at 200 GeV per nucleon [12], using a coefficient of 2.0 for  $p-\bar{p}$  in Eq. 1 and with integral normalized to the number of nucleon participants in Pb+Pb. Within  $|y_{cm}| < 2.5$ , there are  $352 \pm 12$  participant baryons for Pb+Pb and  $52 \pm 3$  for S+S central collisions [12].

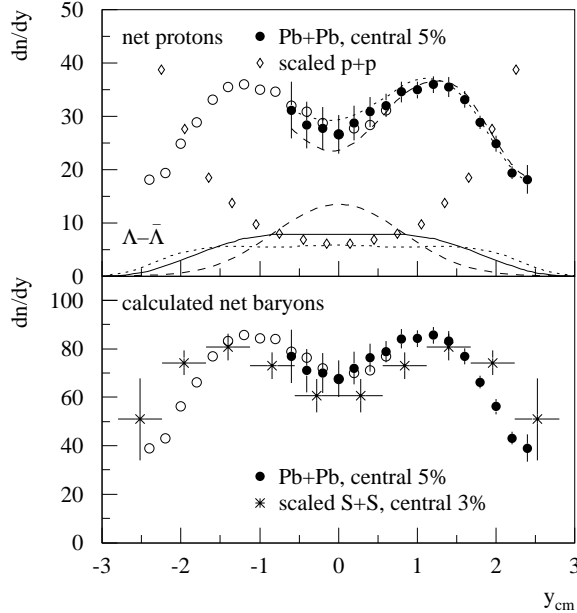


FIG. 1. Upper: normalized rapidity distributions of  $p-\bar{p}$  for Pb+Pb collisions incorporating correction I (open circles are data reflected about  $y_{cm}=0$ , errors not shown). Lines show variation in data using corrections II (dotted) and III (dashed). Also shown are corresponding  $\Lambda-\bar{\Lambda}$  rapidity distributions (I solid, II dotted, III dashed), and the scaled proton distribution for p+p collisions. Lower: normalized rapidity distributions of  $B-\bar{B}$  from Eq. 1 for Pb+Pb incorporating distribution I, and scaled  $B-\bar{B}$  for S+S.

The  $B-\bar{B}$  rapidity distribution is narrower for Pb+Pb than for S+S collisions, indicating increased baryon stopping. (In the CM frame,  $y_{beam} = 2.9$  for Pb+Pb and 3.0 for S+S.) The mean rapidity shift relative to  $y_{beam}$  for participant baryons within  $0 < y_{cm} < 2.5$  is  $\langle \Delta y \rangle = -1.76 \pm 0.05$  for Pb+Pb and  $\langle \Delta y \rangle = -1.63 \pm 0.16$  for S+S collisions.

Fig. 2 shows the event normalized rapidity distribution (assuming pion mass) of  $h^-$  in central Pb+Pb and S+S [12] collisions, and isoscalar inelastic N+N [14] collisions. An independent analysis of Pb+Pb collisions using the NA49 Vertex TPCs found a distribution consistent with these data [21]. The S+S and N+N distributions were scaled relative to that for Pb+Pb by the ratio of the number of participant nucleons and a factor 0.96 to account for the energy dependence of average multiplicities measured in hadronic collisions [22]. No correction for the net isospin difference between Pb+Pb and the other systems was applied. Under the assumption that the net isospin in the final state of a Pb+Pb collision is

carried entirely by mesons, the additional scaling factor needed for comparison of the S+S and N+N distributions to that of Pb+Pb is 1.12.

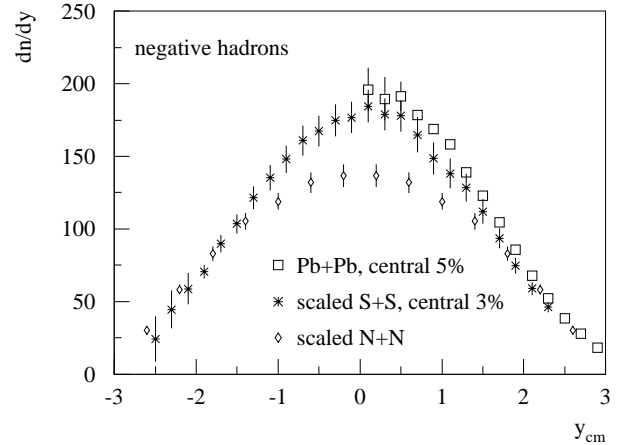


FIG. 2. Normalized rapidity distributions of  $h^-$  for central Pb+Pb collisions, and scaled central S+S and isoscalar inelastic N+N collisions.

The enhancement of meson yield at midrapidity for nuclear collisions relative to N+N collisions has been noted previously [11]. Taking into account the net isospin difference, the agreement between the Pb+Pb and scaled S+S distributions is striking. This scaling of the yield of produced particles with number of participants, first observed in  $p+A$  collisions [23], is also observed in the collision of very heavy ions. Extrapolation of the  $h^-$  yield to full phase space was performed by taking into account the asymmetry in the  $h^-$  rapidity distribution (assuming pion mass) due to the contribution of  $K^-$  [19], resulting in an estimated total  $h^-$  yield of  $715 \pm 30$  particles. The number of  $h^-$  per participant nucleon pair, not adjusted for isospin, is  $4.1 \pm 0.2$  for Pb+Pb collisions, compared to  $3.6 \pm 0.2$  for S+S collisions and  $3.22 \pm 0.06$  for isoscalar N+N collisions [14].

Fig. 3, upper panel, shows transverse mass spectra ( $m_T = \sqrt{m^2 + p_T^2}$ ) near midrapidity for  $h^-$  and  $p-\bar{p}$  for central Pb+Pb collisions. NA49 has previously reported the fit of an expanding hadronic source model [24] to midrapidity  $h^-$  and deuteron  $m_T$  spectra and  $h^-$  correlation functions [6], giving a freezeout temperature of  $T = (120 \pm 12)$  MeV and transverse expansion velocity  $\beta_\perp = (0.55 \pm 0.12)$ . Fig. 3, upper panel, shows the fit of this model with fixed  $\beta_\perp = 0.55$  to the  $h^-$  and  $p-\bar{p}$  spectra reported here. The resulting freezeout temperatures are  $T = (126 \pm 2)$  MeV for  $h^-$  and  $T = (118 \pm 5)$  MeV for  $p-\bar{p}$ .

Fig. 3, lower panel, shows the rapidity dependence of  $\langle p_T \rangle$  calculated within  $0 < p_T < 2.5$  GeV. For  $p-\bar{p}$  for central Pb+Pb collisions,  $\langle p_T \rangle = (825 \pm 37)$  MeV at  $y_{cm} = 0$  and  $(600 \pm 17)$  MeV at  $y_{cm} = 2.4$ , compared to the rapidity-averaged value  $\langle p_T \rangle = (622 \pm 26)$  MeV for central S+S collisions [11]. For  $h^-$  for central Pb+Pb collisions,  $\langle p_T \rangle = (385 \pm 18)$  MeV at  $y_{cm} = 0$ , compatible with  $(377 \pm$

4) MeV for central S+S collisions [12]. (In considering  $\langle p_T \rangle$  for  $h^-$  at high rapidity, note that the kinematic limit for pions for N+N collisions at 158 GeV falls below  $p_T = 1$  GeV near beam rapidity).

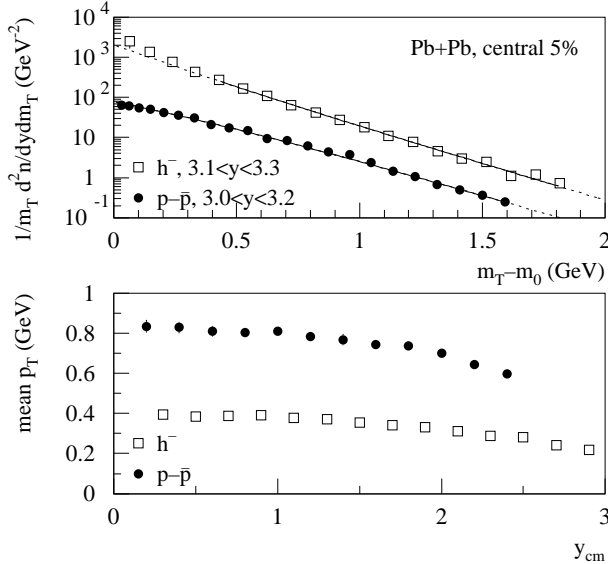


FIG. 3. Spectra for central Pb+Pb collisions. Upper: transverse mass spectra near  $y_{cm}=0$ . Solid lines indicate fits discussed in text; dotted lines are extrapolations of fit function. Lower: rapidity dependence of  $\langle p_T \rangle$  for  $h^-$  and  $p-\bar{p}$ .

A similar characterization of  $p_T$  distributions results from fitting  $(1/p_T) \cdot dn/dp_T$  with a function  $A \cdot \exp(-m_T/T)$ . A fit within  $0 < m_T - m_0 < 0.8$  GeV to the  $p-\bar{p}$  data near midrapidity for central Pb+Pb collisions yielded  $T = (308 \pm 15)$  (NA44 reported  $(289 \pm 7)$  MeV for protons [13]). NA35 found rapidity-averaged  $T = (235 \pm 9)$  MeV for central S+S collisions [12]. The increase in  $T$  and  $\langle p_T \rangle$  with particle mass is consistent with a larger transverse radial flow velocity at midrapidity in Pb+Pb than S+S collisions [6,13].

In summary, baryon stopping for central collisions at ultrarelativistic energies increases with system size. The integrated yield and rapidity density of negative hadrons exhibit scaling with the number of participant nucleons for nuclear collisions, and a small enhancement with respect to N+N collisions. At midrapidity, a large increase is observed in  $\langle p_T \rangle$  for the stopped baryons in Pb+Pb relative to S+S collisions, with no significant increase in  $\langle p_T \rangle$  for negative hadrons. The increase in  $\langle p_T \rangle$  with particle mass is consistent with an increase in transverse radial flow velocity for heavier colliding systems.

This work was supported by the Director, Office of Energy Research, Division of Nuclear Physics of the Office of High Energy and Nuclear Physics of the U.S. Department of Energy under Contracts DE-AC03-76SF00098 and DE-FG02-91ER40609, the U.S. National Science Foundation, the Bundesministerium für Bildung und Forschung, Germany, the Alexander von Humboldt Foundation, the U.K. Engineering and Physical Sciences Research Coun-

cil, the Polish State Committee for Scientific Research (2 P03B 02615 and 2 P03B 9913), the EC Marie Curie Foundation, and the Polish-German Foundation.

<sup>†</sup>deceased <sup>§</sup>present address: Kent State Univ., Kent, OH, USA <sup>#</sup>present address: Physikalisches Institut, Universität Heidelberg, Germany <sup>+</sup>present address: Max-Planck-Institut für Physik, Munich, Germany

- [1] *Proceedings of Quark Matter 96*, ed. P. Braun-Munzinger *et al.*, Nucl. Phys. **A610** (1996).
- [2] N. K. Glendenning, S. Pei and F. Weber, Phys. Rev. Lett. **79**, 1603 (1997).
- [3] T. Alber *et al.*, Phys. Rev. Lett. **75**, 3814 (1995).
- [4] P. Koch, J. Rafelski, and W. Greiner, Phys. Lett. B **123** 151 (1983); K. S. Lee, M. J. Rhoades-Brown, and U. Heinz, Phys. Rev. C **37** 1452 (1988).
- [5] E. Schnedermann and U. Heinz, Phys. Rev. C **50** 1675 (1994); S. Chapman, J. R. Nix, and U. Heinz, Phys. Rev. C **52** 2694 (1995); S. Chapman and J. R. Nix, Phys. Rev. C **54** 866 (1996).
- [6] H. Appelshäuser *et al.*, Eur. Phys. J. **C2**, 661 (1998).
- [7] W. Busza and A. S. Goldhaber, Phys. Lett. **139B**, 235 (1984).
- [8] A. Capella and B. Z. Kopeliovich, Phys. Lett. B **381**, 325 (1996); D. Kharzeev, Phys. Lett. B **378**, 238 (1996); B. Andersson, G. Gustafson, and H. Pi, Z. Phys. C **57**, 485 (1993); M. Gyulassy, V. Topor Pop and S. Vance, nucl-th/9706048, Heavy Ion Physics **5**, 299 (1997); S. E. Vance, M. Gyulassy and X. N. Wang, nucl-th/9806008 (1998), to be published.
- [9] H. Sorge, Phys. Rev. C **52**, 3291 (1995).
- [10] K. Werner, Phys. Rep. **232**, 87 (1993).
- [11] J. Bächler *et al.*, Phys. Rev. Lett. **72**, 1419 (1994).
- [12] T. Alber *et al.*, Eur. Phys. J. **C2**, 643 (1998).
- [13] I. G. Bearden *et al.*, Phys. Rev. Lett. **78**, 2080 (1997).
- [14] M. Gaździcki and O. Hansen, Nucl. Phys. **A528**, 754 (1991).
- [15] M. Aguilar-Benitez *et al.*, Z. Phys. C **50**, 405 (1991).
- [16] S. Wenig *et al.*, Nucl. Instr. and Meth. A **409**, 100 (1998).
- [17] B. Lasiuk *et al.*, Nucl. Instr. and Meth. A **409**, 402 (1998).
- [18] M. Toy, Ph.D. Thesis, UCLA (1998).
- [19] C. Bormann *et al.*, J. Phys. G **23**, 1817 (1997).
- [20] A. Wróblewski, Acta Phys. Pol. B **16**, 379 (1985).
- [21] J. Günther, Ph.D. Thesis, Univ. of Frankfurt (1997).
- [22] M. Antinucci *et al.*, Lett. Nuov. Cim. **6**, 121 (1973).
- [23] W. Busza and R. Ledoux, Ann. Rev. Nucl. Part. Sci. **38**, 119 (1988).
- [24] S. Chapman, P. Scotto and U. Heinz, Heavy Ion Physics **1**, 1 (1995).